



Room 14-0551  
77 Massachusetts Avenue  
Cambridge, MA 02139  
Ph: 617.253.5668 Fax: 617.253.1690  
Email: docs@mit.edu  
<http://libraries.mit.edu/docs>

## **DISCLAIMER OF QUALITY**

Due to the condition of the original material, there are unavoidable flaws in this reproduction. We have made every effort possible to provide you with the best copy available. If you are dissatisfied with this product and find it unusable, please contact Document Services as soon as possible.

Thank you.

**Some pages in the original document contain pictures or graphics that will not scan or reproduce well.**

Comparison of Heat Sink and Fan Combinations  
and Thermal Electric Coolers for use in the  
Mars Gravity Biosatellite

by

Aaron J. Parness

SUBMITTED TO THE DEPARTMENT OF MECHANICAL ENGINEERING IN PARTIAL  
FULFILLMENT OF THE REQUIREMENTS FOR THE DEGREE OF

BACHELOR OF SCIENCE IN MECHANICAL ENGINEERING  
AT THE  
MASSACHUSETTS INSTITUTE OF TECHNOLOGY

[June 2004]  
MAY 2004

© 2004 Aaron Parness

The author hereby grants to MIT permission to reproduce  
and to distribute publicly paper and electronic  
copies of this thesis document in whole or in part.

Signature of Author: \_\_\_\_\_

Department of Mechanical Engineering

May 7, 2004

Certified by: \_\_\_\_\_

John E. Keesee

Colonel, USAF

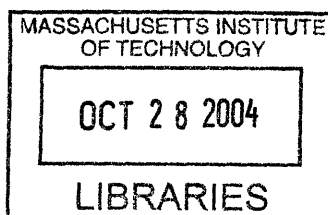
Senior Lecturer and Air Force Liaison

Thesis Supervisor

Accepted by: \_\_\_\_\_

Ernest G. Cravalho

Professor of Mechanical Engineering



ARCHIVES

# Comparison of Heat Sink and Fan Combinations and Thermal Electric Coolers for use in the Mars Gravity Biosatellite

by

Aaron J. Parness

Submitted to the Department of Mechanical Engineering  
on May 7, 2004 in Partial Fulfillment of the  
Requirements for the Degree of Bachelor of Science in  
Mechanical Engineering

## ABSTRACT

An experiment was conducted to help compare possible cooling methods for the payload module of the Mars Gravity Biosatellite. The Satellite will be launched into space with 15 mice on board and rotated to create a 0.38g centrifugal acceleration, the acceleration due to gravity on Mars. The mission will last 5 weeks and take valuable data on mammal's responses to extended periods of time in reduced gravity.

Because of a large heat shield needed for reentering the Earth's atmosphere, the payload module is nearly perfectly insulated. It is therefore necessary to actively transport heat out of the capsule and radiate it off into space. A thermal electric cooler and a heat sink and fan combination were compared in this experiment for that purpose, using a Styrofoam cooler as a model payload.

It was found that the fan and heat sink combination was more efficient than the thermal electric cooler. The coefficient of performances of the respective cooling elements was found to be 5.89 for the fan and heat sink while only 1.67 for the thermal electric cooler. However, it was also observed that the thermal electric cooler, while less efficient, could transport much more heat than the fan and heat sink alone, 26.4 Watts compared to 9.73 Watts in the experimental set up. It has been recommended that a combination of a fan and heat sink be used in the payload module of the satellite.

Thesis Supervisor: John E. Keesee  
Title: Colonel, USAF; Senior Lecturer

## Table of Contents

1. Introduction . . . . .	4
2. Apparatus . . . . .	6
3. Procedure . . . . .	11
4. Theoretical Analysis . . . . .	12
5. Results . . . . .	20
6. Discussion . . . . .	26
7. Conclusions and Recommendations . . . . .	32
8. Appendices . . . . .	33

# 1. Introduction

The thermal analysis and experiment discussed below was undertaken for the specific application in the Mars Gravity Biosatellite Program. The team's primary goal is to study the effects of Martian gravity on mammals. The Project has developed a plan over the last 2 years to launch 15 mice into space on a satellite that will rotate, creating a centrifugal acceleration of .38g thus mimicking the gravity at the surface of Mars. The projected mission length for this satellite is 5 weeks and it is hoped that several of the mice will give birth during the mission. The design of the satellite has been broken up into three parts with each part being developed by a separate university. The Entry, Descent, and Landing System (EDLS) is being worked on at the University of Queenstown in Australia. Students and staff at the University of Washington are designing the BUS portion of the satellite. MIT is working on the Payload module and is also responsible for systems issues.

At MIT, the Payload module has been further divided into a science team, focusing on the experiments to be performed on the mice, and a design team, responsible for designing the interior of the payload capsule. One of the primary requirements for the payload module is the ability to export heat out of the system and onto the BUS for radiation into space. Since the payload is surrounded by a heat shield, used for re-entry purposes, the capsule is nearly perfectly insulated. Computers within the capsule run the controls on the atmospheric filters and pumps, provide adequate living conditions within the cages, and take and store data with cameras and sensors. All of these operations consume power that is dissipated as heat into the air of the capsule. An exothermic reaction within the LiOH filter also creates some heat that must be exported from the payload to maintain a reasonable temperature for the mice. Presently, it is estimated that an average of 80 Watts will need to be exported over the entire length of the 5 week mission. This figure, however, can be expected to fluctuate up to 30 or 40 Watts due to the sporadic use of certain components within the payload. For example, a water pump must be used to supply the mice with fresh water out of an IV bag. Typical gravity valves do not work because of the reduced force. These pumps consume 2 Watts when they are on, so if half of the mice are drinking, the power consumption of the payload increases considerably. Filters, lights, cameras, and other components also run on duty cycles so it important to have a type of feedback control circuit in the thermal exportation system.

The heat that is generated inside the payload goes through a handful of steps before it is radiated into space. Initially, it creates an increase in the air temperature within the payload. That heated air is in contact with the outer shell of the capsule and transfers heat to the shell primarily through convection. The aluminum shell of the payload capsule is in physical contact with a thin aluminum piece of the EDLS system and so heat is conducted from the metal of the capsule to that of the EDLS element. This layer of aluminum is connected to a lightband made by Planetary Systems Corporation. The lightband has two functions. First, the lightband is responsible for the conduction of heat from the EDLS aluminum piece to the BUS base radiator where easy radiation into space is facilitated, and second, it separates the satellite from the BUS system immediately before reentry. The BUS base radiator is the final element in the thermal circuit for the satellite. However, the orientation issues of radiating into outer space are being researched at the University of Washington. The remainder of this paper will focus on the heat transfer from the payload to the lightband only. The heat travels through 4 stages of resistive elements on its way the

lightband. The analysis of these individual elements is presented in a circuit calculation in section 3 of this report, *Theoretical Analysis*.

The second function of the Light Band is to separate the BUS from the Payload and EDLS system directly before re-entry. The Light Band separates non-explosively and the BUS will be left orbiting in space or permitted to burn up in the atmosphere. Thus, the payload will be left with no means of heat exportation and must be able to alternatively maintain a livable temperature for the mice until they are recovered by the land crew in the Australian Outback—where the satellite is supposed to land. A calculation of the air temperature within the payload over time with no heat exportation is shown below in the section, *Theoretical Analysis*, as well.

An effective means to increase the heat transfer rate and control the inner air temperature needed to be designed and tested. The two best methods of boosting the heat transfer in a controllable manner were determined to be installing either a fan and heat sink combination on the interior of the capsule or alternatively, installing a thermal electric device. Both of these apparatuses would work optimally when installed near the outer rim of the capsule, where they would be closest to the capsule—EDLS interface. To better understand the differences between the two methods of cooling, a simple experiment was conceived and executed to provide the necessary data to make a decision.

A Styrofoam container was used to model the payload capsule and two 40 watt light bulbs provided the heat source for the experiment. A thermoelectric cooler was mounted onto the wall of the container as well as a heat sink and fan combination. Each device was attached to an aluminum bar that served to conduct the heat out of the container. The bar's opposite end went into a bucket filled with water and ice and maintained at various cold-side temperatures. Several thermal resistors were surface mounted to the aluminum bar and were used to monitor the temperature gradient. This data was compared for each of the two methods of heat exportation and used to determine which method to implement in the design of the actual satellite. A more detailed description of these components and methods are outlined in the next section, *Experimental Apparatus*.

The results of this experiment proved relevant beyond the specific Mars Gravity Biosatellite application. As the technologies and efficiencies of heat sinks and thermal electric coolers get better, it is important to constantly reevaluate the differences between the two methods. Beyond cooling power, it is critical in aerospace applications to consider power consumption and size requirements. Satellites and spacecraft often have a very limited power supply and the installation of devices can be complicated by complex design structures and restricted working spaces. Several key performance coefficients were obtained and compared during this experiment and the choice, calculation, and explanation of these parameters provides a solid template for anyone wishing to compare the performances of various cooling elements in future space and/or laboratory applications. As NASA ramps up to send a man to Mars, the definition and practice of technology comparison becomes increasingly important. This project has worked to create an effective and practical method for comparisons of thermal elements.

## 2. Apparatus

Two apparatuses were built during the course of this research. The first design failed after several tests were performed. A second, more thoughtful, design was conceived based on the flaws of the first trials and worked effectively for the duration of the data collection.

Both designs had several main features in common. For instance, the primary module of the experiment was a Styrofoam container. This box provided a thermally insulated enclosure that mimicked the payload module. In reality, the Styrofoam allows significantly more heat leakage than would an actual aluminum capsule enclosed in a heat shield, but there were many advantages to using Styrofoam. The material was very easy to machine and manipulate, and was also low cost. Since the leakage was theoretically identical for all trial runs, the term could be ignored.

The first kind of Styrofoam box used was 18 inches by 12 inches by 12 inches. The second apparatus was built with a slightly smaller box, 18 inches by 12 inches by 12 inches at the lid, but only 15 inches by 12 inches by 12 inches at the base. The first box had 1 inch thick walls while the second box's walls measured only  $\frac{3}{4}$  of an inch. Both boxes were outfitted with the equipment necessary to model the thermal circuit in the payload of the real satellite. Two 40 watt light bulbs were used to create a heat source similar to the anticipated 80 watt average during the 5-week mission. These light bulbs were mounted onto a cardboard holder that kept the bulbs upright and also shielded the cooling elements from absorbing any light directly. A Melcor brand extruded aluminum heat sink of dimensions 4.125 inches by 4.125 inches was mounted onto the wall of the box. A piece of 6061 aluminum bar stock, 3 inches by a  $\frac{1}{2}$  inch in cross section and 6 inches in length, was attached to the back of the heat sink and came out through a fitted hole in the Styrofoam. This piece of bar stock was bolted to another piece of aluminum and inserted into a cold water bath that was assumed to be an infinite cold reservoir. The aluminum bar stock was wrapped in packing foam to reduce convection and mimic the pure conduction heat transfer process that occurs in the vacuum of space. A 4.72 inch Panaflo fan was matched to the heat sink and positioned so that air was pushed through the fins of the aluminum when the fan was turned on. Power was supplied by a standard adjustable power supply.

The second cooling device that was built into the Styrofoam was a thermo electric device also from Melcor. The cooler was 1.57 inches by 1.57 inches in size and its spec sheet can be found in Appendix A. This cooler was slathered with thermal grease and pressure fitted between two half inch slabs of aluminum. A piece of aluminum bar stock, 3 inches by  $\frac{1}{2}$  inch by 6 inches, identical to that used with the heat sink, was mounted to the hot side slab of aluminum and protruded through a second hole in the Styrofoam. This piece was also wrapped in packing foam to limit convection, and connected to an identical second piece of aluminum, which was inserted into the same cold water bath as before. The thermo electric device also ran off of the standard adjustable power supply. The second design of the apparatus included some modifications to the mounting of the thermal electric cooler. First of all, two coolers were mounted in series between the plates. The fixture was also countersunk into the Styrofoam so that the hot side of the plate was actually in the wall of the cooler. Insulation was wrapped between the hot aluminum fixture and the cold aluminum fixture to limit the thermal exchange between the two and the Panaflo fan was blown across the cool side of the fixture to increase the convection from the hot air to the thermal electric device's fixture. To aid this convection even further, a small black heat sink was connected to the cold

side of the heat sink. The connection was made as firm as possible and used thermal grease to minimize any losses in the joint. A black heat sink was chosen to increase the radiation that the heat sink absorbed. Thermal grease was also applied to all of the aluminum joints outside of the Styrofoam box before the second collection of data occurred. This reduced the heat loss that was observed at the joints in the first set of data. A picture of the thermal electric device apparatus and the heat sink and fan combination is shown below in Figure 1. The heat sink used with the fan can be seen on the left, it is silver, while the thermal electric cooler was mounted behind the black heat sink shown on the right of the figure.

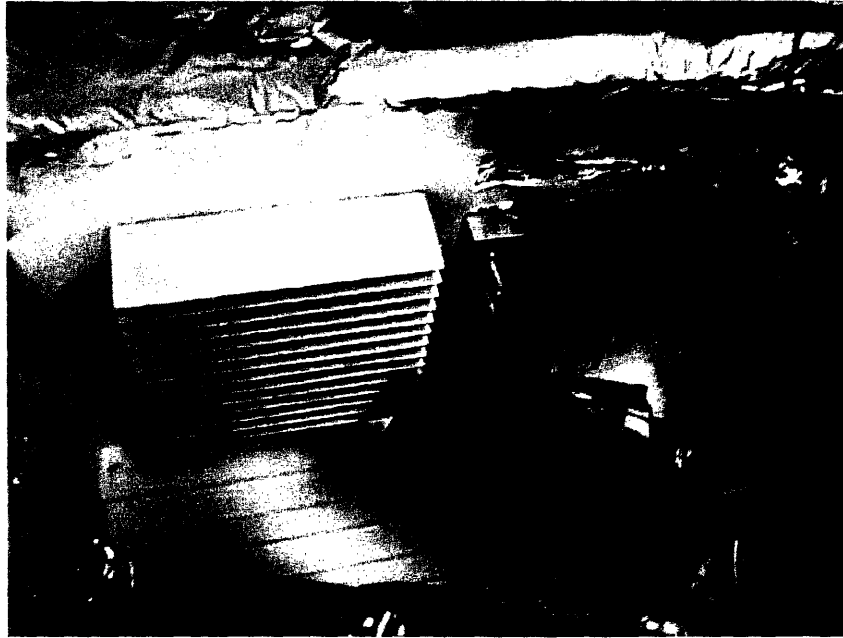


Figure 1: Thermal electric cooler apparatus with modifications as well as heat sink and fan combination

Several safety precautions were taken in the second experimental design as well. Tin foil was placed on the lid and upper walls of the Styrofoam box to reduce radiation from the light bulbs and to keep the Styrofoam from melting. A cup of water was put inside the box in both designs. This feature added thermal mass to the system and prevented a sudden rise in heat that might cause fire or melting. Despite this, the first experiment melted all the way through the lid as shown below in Figures 2 and 3.



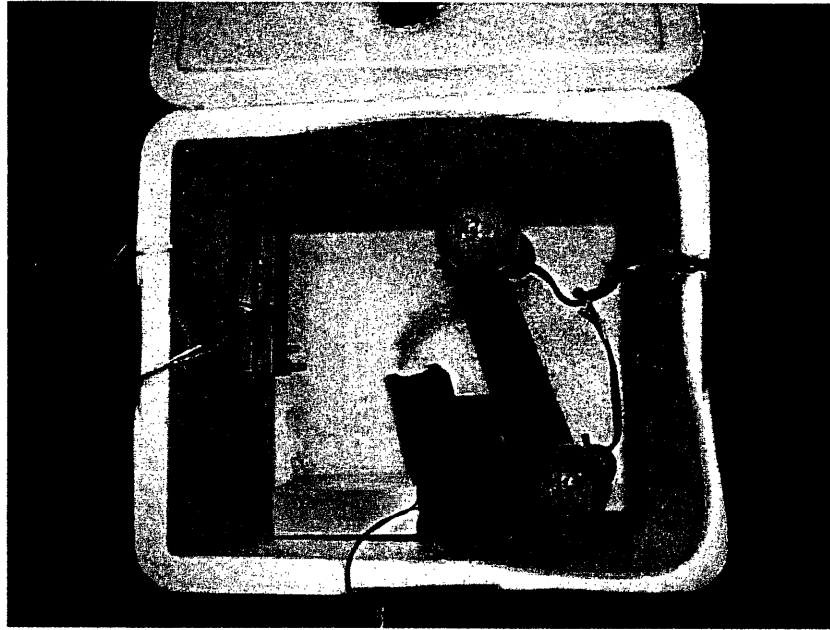


Figure 2: First experimental apparatus box after failure due to melting



Figure 3: Lid of first experimental apparatus after failure due to melting

Figures 4 and 5 show the second experimental apparatus that functioned without any serious problems.

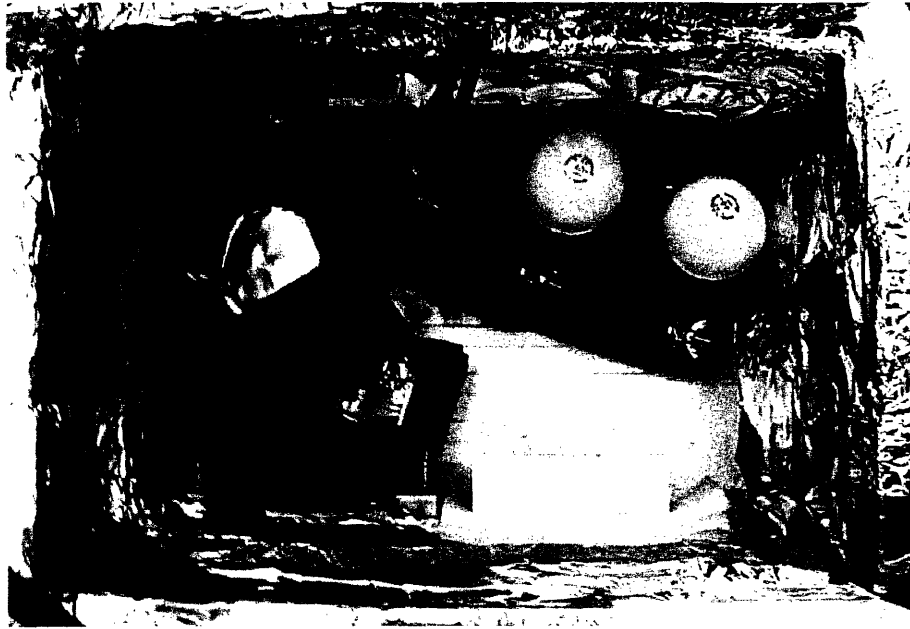


Figure 4: Improved experimental apparatus, inside the Styrofoam box

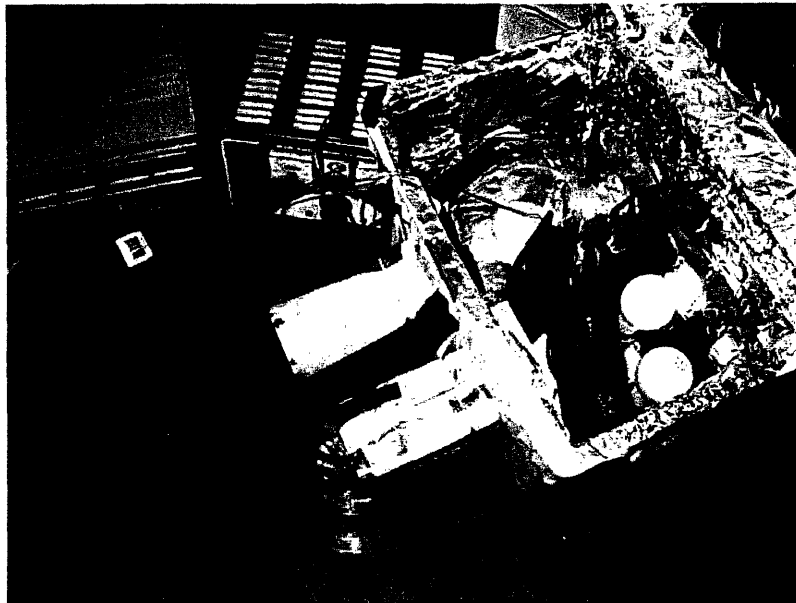


Figure 5: Improved experimental apparatus; overhead view

A Stanley brand non-contact infrared thermometer was used to acquire data. This device shoots an infrared wave onto an object and is able to remotely measure the temperature. A laser pointer guides the user and ensures that the correct surface is being measured. The digital display on the thermometer reported temperatures in  $\frac{1}{2}$  degree C increments. The device had a distance to spot size ration of 6:1. Figure 6, below, is a picture of the thermometer.



Figure 6: Stanley noncontact infrared thermometer on aluminum bar stock

### 3. Procedure

The purpose of this experiment was to compare the thermal cooling abilities of two separate methods at steady state conditions. Since the mission length is projected at 5 weeks, the transient responses of each system were largely ignored. Therefore, the first step taken before data collection was heating the box. The light bulbs were switched on and given sufficient time (about 10 minutes) to heat the Styrofoam container. Equilibrium was reached at the point where the heat generation of the light bulbs equaled the heat losses through the walls and joints of the box. The first kind of data set taken was for natural convection across the heat sink. The cold bath was set and the aluminum bar stock inserted into the water. Temperature measurements were then recorded along the horizontal aluminum bar stock every  $\frac{1}{2}$  inch using the spot thermometer. Temperature readings were also taken for the water bath, the outer wall of the Styrofoam at a specific spot far from the heat source, the inner wall of the Styrofoam at the same point far from the heat source, the top of the heat sink, and the top of the black plastic casing for the Panaflo fan. The steady state temperature of the cup of water inside the box was also recorded. This data can be found in Appendix B.

For the next data set, the Panaflo fan was wired to the power supply and turned on. Several minutes were spent waiting for the system to reach a new steady state, and then the same temperature readings were taken. Several cubes of ice were added to the cold water bath to ensure that the temperature remained as consistent as possible across the various trials. This data is also presented in Appendix C.

The third trial was run using the thermal electric cooler. The cold water bath was switched over to the other side of the apparatus and the fan was reoriented so that it blew across the thermal electric cooler's heat sink. The leads from the thermoelectric cooler were connected to a second power supply and the device was turned on. Once again, the system was allowed to reach steady state before any data was taken. Because of the screw heads used in pressure fitting the thermoelectric cooler, only  $5\frac{1}{2}$  inches of aluminum bar stock protruded from the Styrofoam container in the first design. However, in the second apparatus, with the cooler mounted coincident to the Styrofoam wall, a full 6 inches of data was taken. All of the measurements recorded for this third type of trial are presented in Appendix D.

Two distinct sets of data are presented in the appendices. The first set is from the 1<sup>st</sup> experimental design. The cooler was run with two 100 watt light bulbs in an effort to create greater temperature gradients for measurement. The second set of trials was undertaken at as close to the satellite application's conditions as possible. Two 40 watt light bulbs were used and a fan was run across the thermal electric cooler's cold plate. Several trials were repeated at each of the various conditions to ensure the consistency of the data. These repeated trials also provided enough data to do an error analysis. The system was allowed to cool all the way down to ambient temperature between sets of trials and the order in which each trial was performed was varied. All of the data is presented in the trials' respective appendices, B, C, and D.

Ambient room temperature was also recorded before and after each trial as well as Styrofoam wall thickness and the water temperature inside the Styrofoam box.

## 4. Theoretical Analysis

A diagram of the interface between the payload module and the bus base radiator is shown below in Figure 7. It is useful to understand the larger thermal circuit into which the cooling elements that were tested will be implemented. Therefore, the first analysis performed is a calculation of heat transfer through the various thermal resistances that exist between the payload module and outer space. Preliminarily, this will be performed without considering any of the possible cooling elements.

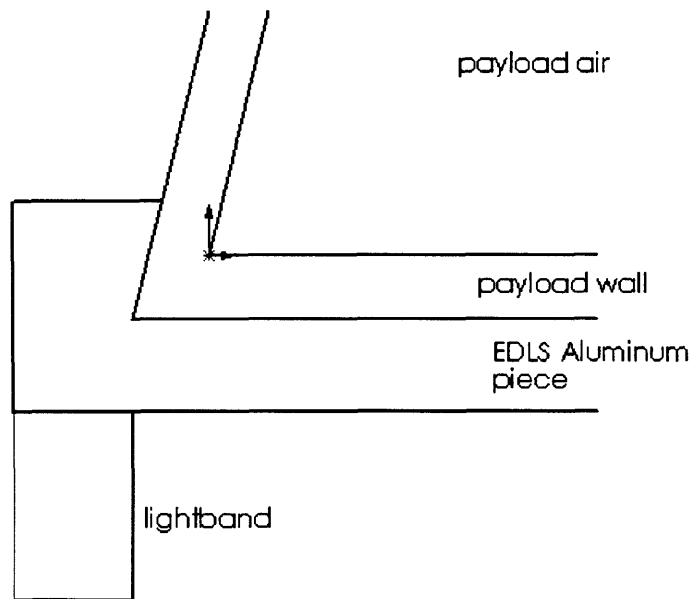


Figure 7: Diagram of the thermal circuit from payload to outer space

Assuming a payload air temperature of 20°C, which is a system requirement dictated by the science team, and a heat transfer rate of 80 watts, which must be achieved to keep the inner air temperature constant, the temperature at each element in the circuit can be calculated, and most importantly, the temperature at the end of the lightband. If this number does not match the temperature at which 80 watts will be radiated into space, then the thermal resistance of the circuit must be adjusted. If the temperature at the end of the lightband is too high, then more energy will be radiated out into space than required, cooling the air inside the payload. The opposite of this, however, is more likely. If the temperature of the bus base radiator is too low with natural convection alone, then 80 watts will not be radiated into space and the payload will heat up, endangering the mice. The 80 watt rate of dissipation into space must be maintained and controlled.

Another effect that is being considered by the team at the University of Washington is the effects of radiation from the earth and or the sun. The temperature of space that the radiator interacts with varies significantly if the radiation plates are sun facing or in shadow.

The planned orientation of the satellite is such that the Bus will always be earth facing during the mission.

The thermal resistances of each element must be assessed, as shown below.

### Thermal Resistances

$$R_{\text{conv air-payload}} = 1/(h_c * A_{\text{payload}}) \quad (1)$$

$$R_{\text{cond payload}} = t_p / (A_{\text{payload}} * k_{\text{aluminum}}) \quad (2)$$

$$R_{\text{cond EDLS}} = t_{\text{EDLS}} / (A_{\text{EDLS}} * k_{\text{aluminum}}) \quad (3)$$

$$R_{\text{cond LB}} = t_{\text{LB}} / (A_{\text{through}} * k_{\text{aluminum}}) \quad (4)$$

In these equations, R equals the thermal resistance (K/W),  $h_c$  is the convection coefficient in (W/(m<sup>2</sup>\*K)), A represents the cross sectional area (m<sup>2</sup>), t is the thickness of the element (m), and k is the thermal conductivity (W/(m\*K)). After consulting with Planetary Systems, it was decided to model the conduction across the lightband as steady conduction through the ¼ - 28 fasteners that attached the two parts of the band. The lightband is 2.1 inches thick and has a total of 60 fasteners in the lightband, which has a diameter of 38.810 inches. The thickness of the EDLS system is approximately ½ an inch and the contact area is roughly 330 square inches. The cross sectional area of the payload base is approximately 1134 square inches. The actual dimensions of the satellite are not set in stone at this point, but these numbers are close enough to do a worthwhile analysis. Also, the method of calculation is good no matter the dimensions. Other numbers can very easily be substituted into the following equations. Further, since the primary importance of this experiment is the cooling element to be installed between the payload air and the payload wall, the thermal resistances of the other elements in the system are non-critical, as long as they remain the same for all trials and assumptions.

The most difficult resistance to calculate in the thermal circuit without cooling elements present was the convection term. The convection coefficient,  $h_c$ , was calculated using the following Nusselt correlation for natural convection with laminar flow on a vertical wall which holds for Rayleigh numbers less than 10<sup>9</sup>,

$$Nu_L = .68 + .670*(Ra_L * \Psi)^{.25}, \quad (5)$$

$$\Psi = [1 + (.492/Pr)^{.9/16}]^{-16/9}, \quad (6)$$

where  $Ra$  is the Rayleigh number and  $Pr$  is the Prandtl number. The Rayleigh number is calculated from the following equation,

$$Ra_L = Gr * Pr = B * \Delta T * g * L^3 * \mu * c_p / (v^2 * k), \quad (7)$$

where B is the coefficient of thermal expansion (1/K),  $\Delta T$  is the difference in temperature of the two surfaces (K), g is the gravitational constant (m/s<sup>2</sup>), which in our case is .38 \*  $g_{\text{earth}}$ , L is the length of the wall (m),  $\mu$  is viscosity of the fluid (kg/(m\*s)),  $c_p$  is the heat capacity of the fluid at constant pressure (J/(kg\*K)), and v is the kinematic viscosity (m<sup>2</sup>/s). Assuming the

acts like an ideal gas, B is simply 1/T, which is .00341 \* 1/K in our system. ΔT is only on the order of several Kelvin, g is 3.728 m/s<sup>2</sup>, and L is approximately the diameter of the payload, which equals 38 inches. The viscosity of air at 20°C is 1.825E-5 kg/(m\*s), the heat capacity is 1006.4 J/(kg\*K), and the kinetic viscosity is 1.535E-5 (m<sup>2</sup>/s). The k value for air is .025 W/(m\*K). Plugging all of these values into the equation, it is found that the Ra number is very much less than 10<sup>9</sup> for all possible conditions in the payload module, it is 9.81E6 for the values listed above.

The Prandtl number is found using the following equation:

$$Pr = \mu * c_p / k . \quad (8)$$

The value of the Prandtl number is 0.72 for air.

Therefore the Nusselt correlation holds and the convection coefficient, h<sub>c</sub>, is calculated using

$$h_c = Nu * k / L, \quad (9)$$

and found to be 10.61 W/(m<sup>2</sup>\*K).

It can be seen that the laminar flow assumption is valid by evaluating the Reynolds number,

$$Re = \rho * v * D / \mu . \quad (10)$$

For the air in the payload, with a density of 1.20 kg/m<sup>3</sup>, diameter of 38.1 inches, and viscosity of 1.825E-5 kg/(m\*s). requires an air velocity of over 1 m/s to invalidate the assumption of laminar flow. This is unlikely to occur during natural convection, with no fans or blowers forcing air across the base of the capsule.

Using the convection coefficient along with the dimensions and properties of the system, the thermal resistances are found to be as follows,

$$R_{conv \text{ air-payload}} = 1 / (h_c * A_{payload}) = 0.4428 \text{ } ^\circ\text{C/W} \quad (11)$$

$$R_{cond \text{ payload}} = t_p / (A_{payload} * k_{aluminum}) = 0.000098 \text{ } ^\circ\text{C/W} \quad (12)$$

$$R_{cond \text{ EDLS}} = t_{EDLS} / (A_{EDLS} * k_{aluminum}) = 0.00034 \text{ } ^\circ\text{C/W} \quad (13)$$

$$R_{cond \text{ LB}} = t_{LB} / (A_{through} * k_{aluminum}) = 0.0102 \text{ } ^\circ\text{C/W} \quad (14)$$

An equivalent resistance of 0.4534 °C/W is obtained by adding all of these individual resistances. It is a simple summation because all of the thermal pathways are in series and not in parallel. Assuming a heat transfer rate of 80 watts, the outer temperature of the lightband can be calculated using the following equation:

$$Q' = (T_{payload \text{ air}} - T_{outer \text{ LB}}) / R_{eq} . \quad (15)$$

The temperature at the lower edge of the lightband is -16.28 °C.

This result shows that a cooling device is necessary to decrease the thermal resistance and thereby increase the temperature at the lower edge of the lightband. The temperature of the lower edge of the lightband must match the Bus specifications if the payload module temperature is to remain at 20°C throughout the mission, requiring an average of 80 watts is to be pumped out of the system. As mentioned in section 1, *Introduction*, the two primary methods of increasing the heat transport being considered are a fan and heat sink combination or a thermal electric cooler.

We can calculate the expected velocity of air necessary in the payload if we hoped to dissipate 80 watts by forced convection. Due to space constraints, only a 4 inch by 4 inch duct is available for heat sinks and fans. If a 14 fin extruded aluminum heat sink is placed around the entire circumference of the payload (3.03 meters), and air is blown across it, heat will be transferred out of the system. The pertinent question is how fast will the air have to be blown? Modeling the system as 13 small rectangular ducts, 0.029 meters x 0.1016 meters, we can use the Nusselt correlations for laminar and turbulent flow with fully developed hydrodynamics and heat transfer to approximate the required air velocity. Equation 10 defines the Reynolds number, which in our case becomes  $Re = 903 * v_{air}$ . The Nusselt correlation for laminar flow,  $Re < 2800$ , is as follows:

$$Nu = 7.54 + \frac{0.03 * (D_h/L) * Re_{Dh} * Pr}{1 + 0.016 * [(D_h/L) * Re_{Dh} * Pr]^{0.666}} \quad , \quad (16)$$

where  $D_h$  is the hydraulic diameter (m). However, for air velocities above 3 m/s, the flow becomes turbulent in the channel and an alternative Nusselt correlation must be used. The turbulent flow equation is below:

$$Nu = \frac{(f/8) * (Re_{Dh} - 1000) * Pr}{1 + 12.7 * (f/8)^{0.5} * (Pr^{0.666} - 1)} \quad , \quad (17)$$

$$f = (0.790 * \ln(Re_{Dh}) - 1.64)^{-2} \quad , \quad (18)$$

where  $f$  is the nondimensionalized friction factor. This correlation holds for  $3000 < Re_{Dh} < 10^6$  and  $0.5 < Pr$ .

Using a hydraulic diameter of 0.0135 meters, a length (circumference) of 3.03 meters, and a Prandtl number of 0.72 for air, the Nusselt numbers can be calculated as the air velocity varies. Using equation 9, the convective heat transfer coefficient can be solved for, then plugging into equation 15, a heat transfer rate can be obtained. In equation 15, we assume that there is a 2°C temperature difference between the outer payload wall and the temperature of the air. These temperatures are assumed to be steady state and therefore constant. Looking at air velocities from 0 m/s up to 22 m/s gives a good sense of how the heat transfer rate depends on the power of the fan in the thermal system. The calculation results are presented below in Figure 8.



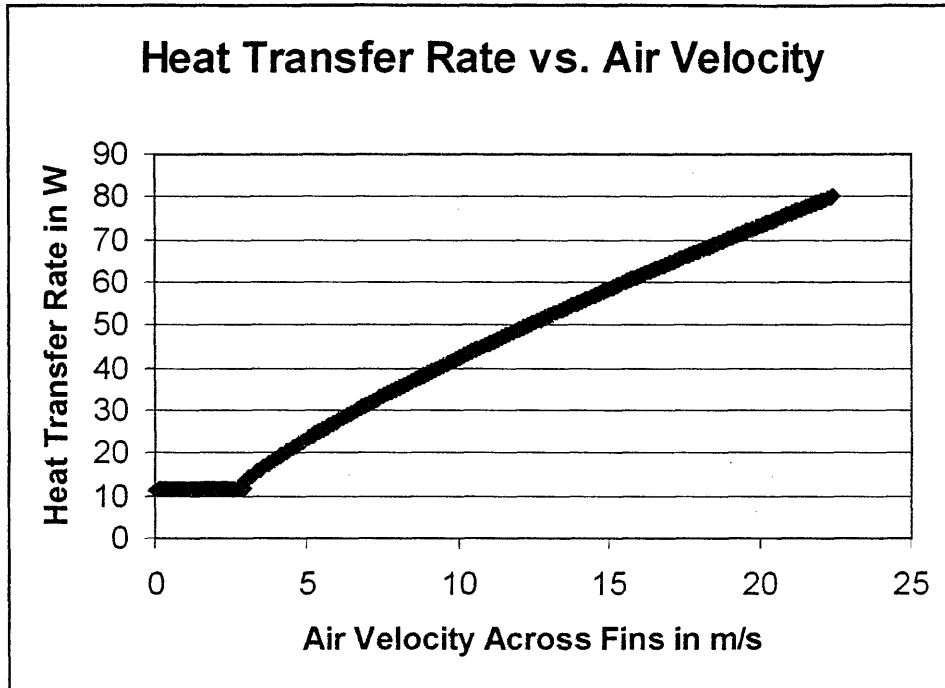


Figure 8: Calculated heat transfer rate for forced convection against air velocity

The relatively flat section to the left of the graph is the laminar flow region of the graph while the curve that takes up most of the graph is for turbulent flow velocities. This figure shows that to export 80 watts of heat, the fans inside the payload would have to force air through the heat fin channels at over 20 m/s. This is unfeasible for a 4 inch by 4 inch fan. Therefore, alternative methods of cooling must also be considered.

It is useful to model the two methods of heat transfer as they apply to the experimental set up in the Styrofoam box. Which method appears to function most efficiently and can increase the heat transfer rate the necessary amount?

In the experiment undertaken, significant losses of heat occurred through the Styrofoam wall of the container. The heat moves from the air in the box to the inner wall of the Styrofoam through natural convection, then through the Styrofoam wall by conduction, and finally into the atmosphere by natural convection off the outer surface of the box. Taking the observed value of about 63°C (temperature of the water in the cooler for the first apparatus operating with two 100 watt light bulbs) as the steady state temperature of the air in the box, this circuit can be calculated. The inner wall of the box was measured when no cooling element was activated. The outer wall was also measured. Therefore, the loss of heat through the wall can be quantified by simple calculation. The Styrofoam box's outer wall temperature was measured as 36°C, whereas the inner wall was measured at 73.5°C. The total surface area of the Styrofoam box that was exposed to the air was 1104 inches<sup>2</sup> and the Styrofoam wall was 1 inch thick. Using Fourier's Law of Cooling and using the value of Styrofoam's thermal conductivity, .0027 W/(m\*K), we can quantify these losses without calculating the convection coefficients as follows:

$$Q'_{\text{loss}} = A_{\text{styrofoam}} * k_{\text{styrofoam}} * (T_{\text{inner wall}} - T_{\text{outer wall}}) / t_{\text{wall}}, \quad (19)$$

which gives a value of 2.80 watts for  $Q'_{\text{loss}}$ . Comparing this to the 200 watts being generated by the light bulbs, the loss of heat through conduction by the Styrofoam walls is very small.

There are, however, other losses that exist within the apparatus which are more difficult to quantify. The lid of the Styrofoam box does not seal perfectly to the walls, and thus heat seepage will occur. Also, the plastic handles of the cooler have a higher value of thermal conductivity than the Styrofoam, and are also colored black, which increases their absorption of heat through radiation. Heat seeps out through the cooling element that is not activated at a slow rate also. For instance, when the fan and heat sink is being tested, air is circulating across the thermal electric cooler's heat sink as well. Although the thermal electric cooler is not coupled with a cold water bath, some heat transfer occurs through the aluminum and to the ambient air outside the box

Next is the examination of the heat sink and fan combination that was added to the Styrofoam box to provide greater heat transfer rates. The heat transfer of a single fin on a heat sink can be computed using the following equation for a convective heat transfer with an adiabatic tip condition:

$$q_f = M * \frac{[\sinh(mL) + (h/(m*k))*\cosh(mL)]}{[\cosh(mL) + (h/(m*k))*\sinh(mL)]} \quad (20)$$

with

$$m^2 = h * \text{perimeter} / (k * A_{\text{cross section}}), \quad (21)$$

$$M = [h * \text{perimeter} * k * A_{\text{cross section}} * (T_b - T_{\text{ambient}})]^{1/2}. \quad (22)$$

This is a cumbersome expression and must be summed over all 14 fins and coordinated with the 0.312 inch thick base plate. Instead, the rest of the heat sink and fan analysis will use a given thermal resistance on the spec sheet of the heat sink. The thermal resistance of the heat sink is 1.3°C/W for the condition of natural convection at 25°C and a 100 Watt load. This closely mimics our conditions of an 80 Watt load and 38°C average temperature inside the Styrofoam box for the second apparatus.

The thermal resistance of the aluminum bar is found using equation 3 but applied to the aluminum bar that protrudes out the side of the box. Since the aluminum bar stock used in the actual experiment is 6061 aluminum and not the 7075 aluminum used in the payload modeling, a thermal conductivity value of  $k = 167.3 \text{ W}/(\text{m} * \text{K})$  was used. A 0.944°C/W thermal resistance was found for the aluminum bar stock. The thermal resistance of the bar that enters the cold bath is very similar, except that it emerges above the water bath only 1.5 inches. Its thermal resistance is 0.236°C/W.

This second piece of aluminum is immersed 4 inches deep in a cold bath that we can model as an infinite cold source at constant temperature. The water bath was stirred frequently to minimize any insulative boundary layers that might form and reduce heat transfer. Thus at steady state, the aluminum that is immersed will also be constant and near the temperature of the cold bath. This creates a circuit with known end point temperatures that allows for the prediction of heat transfer through the aluminum bar. Solving for the equivalent resistance,

$$R_{eq} = R_{\text{heat sink conv}} + R_{\text{horizontal alum cond}} + R_{\text{vertical alum cond not immersed}} \quad (23)$$

yields a result of  $R_{eq} = 2.48^{\circ}\text{C}/\text{W}$ . This result corresponds to a  $Q'$  of 15.32 watts when the temperature of the air inside the Styrofoam box is  $38^{\circ}\text{C}$  and the cold water bath has a constant temperature of  $0^{\circ}\text{C}$ .

When the fan is turned on and supplied with 12 Volts at .15 Amperes, the heat transfer rate increases significantly. By running the hot air over the heat sink, the thermal resistance of that particular element is reduced. This could result in as low an equivalent resistance as  $1.18^{\circ}\text{C}/\text{W}$  if the heat sink resistance was completely overcome, which correlates to a  $Q'$  of 29.66 watts. This is over a 100% increase in the cooling power of the system. Section 5, *Results*, presents data that corresponds to this variation and section 6, *Discussion*, compares this theory with the data obtained.

Using a thermoelectric cooler is an alternative method of increasing the heat transfer rate out of the Styrofoam box. The two sides of the device sustain a temperature difference when supplied with electrical power. The Melcor PT series cooler tested in the experiment operated at a maximum voltage of 14.4 volts with a current of 8.5 amps, although in practice, it never required so much current. At those conditions, the device maintains a  $64^{\circ}\text{C}$  temperature difference from hot side to cold side. The ideal operating temperature for the device is  $T_h = 25^{\circ}\text{C}$ , when  $T_h$  is the hot side of the device. This condition was not possible to meet in the experiment, so the device consequently never ran to its full potential. The thermal electric cooler was mounted between two plates of aluminum with the hot side closest to the wall of the Styrofoam box. The Panaflo fan was positioned to blow the hot air in the box across the cold side of the mounting. This allowed for greater heat transfer and allowed the thermal electric cooler to pump out heat more efficiently. This concept can be understood better with an analogy. Put an ice cube in a hot box and it will not lower the temperature, but put an ice cube in a box and blow the air around it, the ice cube will melt much faster and have a higher thermal transfer rate. The same principle is true for thermal electric devices. The thermal electric device pumps a maximum of 72 watts at optimal conditions, but in our situation, it is expected that the device will only achieve about 45 watts. This corresponds to a temperature of  $52.4^{\circ}\text{C}$  at the interface between the aluminum bar and the fixture of the thermal electric device. This data was taken in the experiment and is presented in section 5, *Results*, and compared with the theory in section 6, *Discussion*.

It is important to note, however, that this result predicts that the thermal electric cooler will perform better than either the heat sink alone or the fan and heat sink combination.

Another calculation must be performed to ensure the safety of the mice from overheating during the reentry, landing, and recovery of the satellite. After the light band separates the Bus from the Payload and EDLS systems, there will be significantly less surface area that is radiating heat into space. With this final element in the thermal circuit no longer attached to the payload, the ability to export heat will be severely decreased. The payload capsule will start to store its heat in the latent energy of the air. The pertinent question is how long will it take for the payload to become unreasonably hot for the mice to survive. That time must be less than the time it takes for reentry, landing, and recovery of the mammals if the mission is to be a complete success.

Under ideal conditions, all systems would be allowed to operate as normal during this final phase of the mission, but there are some non-vital systems that can be turned off to

reduce the amount of heat created after separation. The lights inside the payload, for instance, do not have to remain on, nor do the water pumps need to be operational as the mice should have enough water in their water bottle bladders to last until recovery. Certain atmospheric sensors may be allowed to turn off or run on duty cycles during the reentry and landing process. Even so, not all systems can be shut down completely, so a good approximation is that the payload will be operating at 40 watts after separation and until recovery.

Another precaution that can increase the amount of time that the temperature remains livable for the mice is to reduce the temperature significantly immediately before separation. Starting from with a cold payload will prolong the time until overheating by adding an extra amount of power required to heat from the cold payload back up to the steady state condition of 20°C. For this step, it is assumed that the mice will be unharmed by cooling the payload to 10°C prior to separation and that the cooling elements in position have sufficient power to obtain this temperature when the system has reduced the heat generation from 80 watts to 40 watts. Another assumption is that the mice will survive the reentry, landing, and recovery process at temperatures up to 30°C.

Taking the amount of air in the payload to be approximately 2.87 m<sup>3</sup>, which was calculated by subtracting the large solid elements from the total volume of the capsule, we can do a simple calculation using the thermal capacitance of air. We can use the expression,

$$Q = m \cdot c_p \cdot \Delta T \quad (24)$$

where m, the mass of a given element in the system (kg). This expression can be applied to all of the large elements in the system to see how much total heat must be added to the system to increase the air temperature to 30°C. For air, Q was found to be about 30,700 Joules using  $\rho = 1.20 \text{ kg/m}^3$  for the density of air and converting the volume into mass. The 25 kg of filters require approximately 1,250,000 Joules of heat. The 15 kg of metal and plastic require approximately 360,000 Joules while the 8 kg of electronics and sensors require an additional 320,000 Joules. The batteries weigh 9 kg and require approximately 165,000 Joules. Adding all of these thermal masses together, the payload system requires 2,125,700 Joules of energy to increase in temperature from 10°C to 30°C. Running the payload at 40 watts and using the following relationship,

$$\text{time to overheat} = Q / Q'_{\text{reduced}}, \quad (25)$$

shows that the reentry, landing, and recovery process must take less than 53,142 seconds or about 14 hours. This result is only a first order approximation, but it shows the real danger of overheating the mice during the reentry to recovery process. Some alternative ways of cooling the system may be required to ensure the well being of the mice. These alternatives are briefly discussed in section 7, *Conclusions and Recommendations*.

## 5. Results

The first set of data taken was for the heat sink alone in the first experimental apparatus, when there were two 100 watt light bulbs in the Styrofoam box. The temperature gradient across the aluminum is shown below in Figure 9.

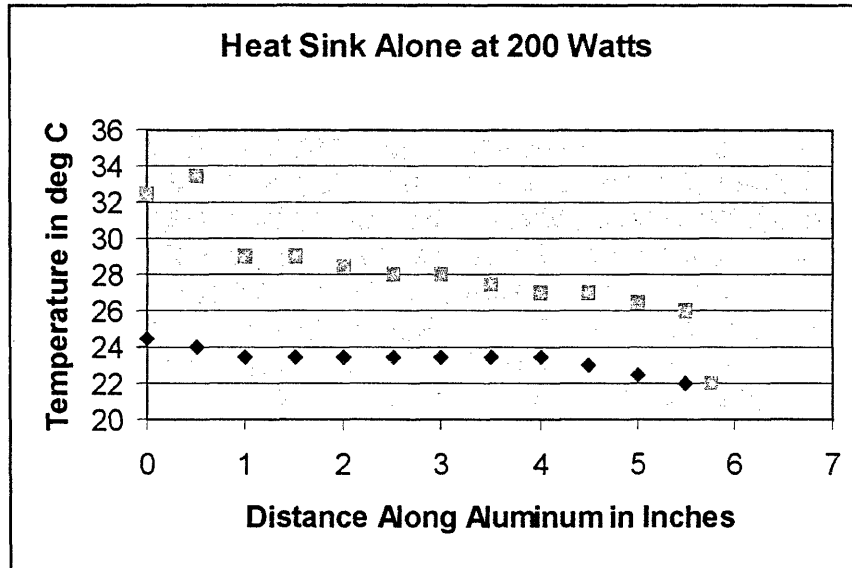


Figure 9: Heat sink data taken for two trials at 200 watts (first apparatus)

The lower set of data is significantly lower than the higher set, primarily because insufficient time was given for the system to reach steady state. The upper data set shows a trial after the light bulbs had been on for nearly an hour and the air inside the box had reached its peak temperature. It is also important to note that the water bath temperature varied for these two trials; the upper data set had a water bath of  $5^{\circ}\text{C}$  while the lower trial had a significantly colder water bath,  $-0.5^{\circ}\text{C}$ . Although every effort was made to maintain a constant water bath temperature, the ice had already started to melt by the time the second trial was run and it was impossible to achieve the same low temperature water bath without restarting the entire process with a fresh bag of ice. The top of the heat sink inside the cooler increased slightly from the first trial to the second, jumping from  $39.0^{\circ}\text{C}$  for the blue dots to  $40.5^{\circ}\text{C}$  for the upper data set.

The next set of data presented in Figure 10 is for the heat sink and fan combination. The fan was run off of a power supply at 12 volts and .15 amperes of current. The data confirms an increase in the cooling power of the heat sink as predicted by section 4, *Theoretical Analysis*. This can be seen below in the higher temperature drop across the same aluminum bar.

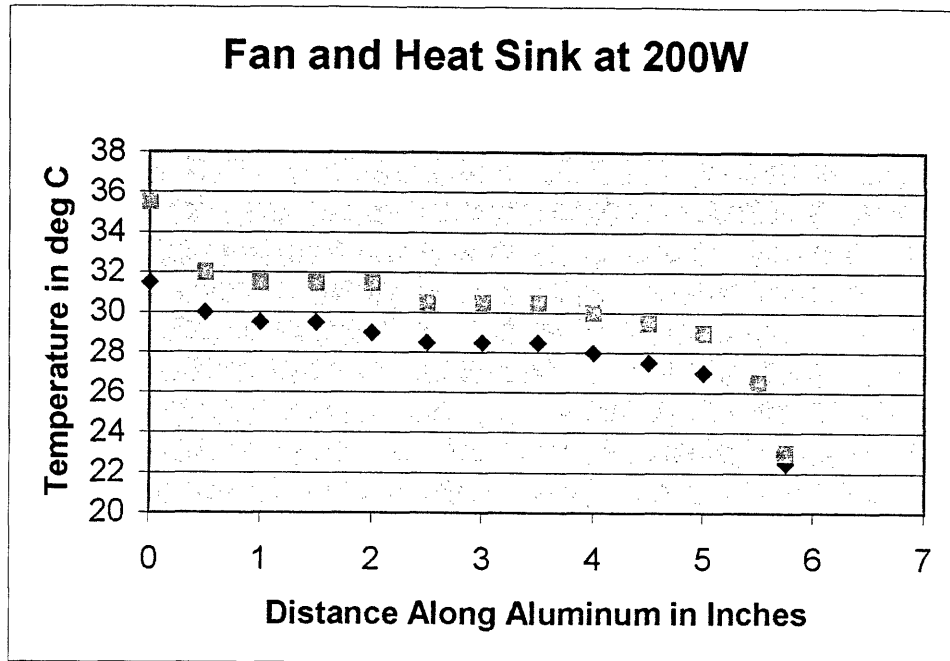


Figure 10: Fan and heat sink data taken at 200 watts (first apparatus)

Here there is a much greater consistency between the data sets because steady state was reached in both cases. The temperature of the top fin on the heat sink was recorded at 42°C and 43°C for two trials respectively. These temperatures are higher than those of the heat sink alone because the fan was blowing hot air across the heat sink, which naturally transferred more heat to the aluminum resulting in a higher temperature measurement. The water bath temperatures differed for these two trials, rising from 0.5°C to 6.5°C over the time between data sets.

The third trial run at 200 watts was for the thermal electric cooler. The data is presented below in Figure 11.

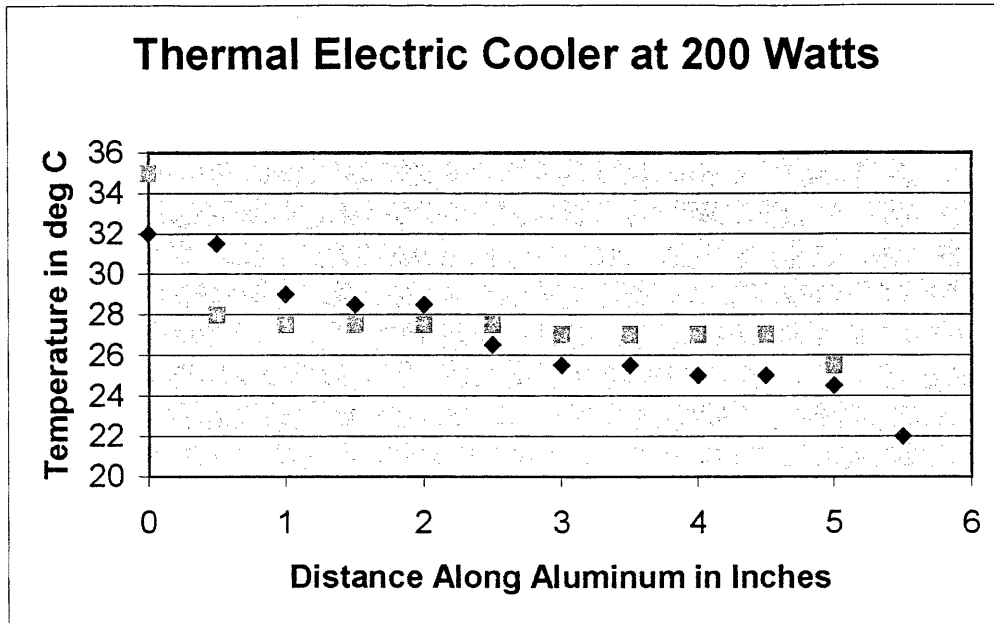


Figure 11: Thermal electric cooler data at 200 watts (first apparatus)

This data also shows an improvement over the heat sink working alone to cool the Styrofoam box as was predicted in section 4, *Theoretical Analysis*. The two data sets cross over one another twice, at 2.5 inches and 0.5 inches down the aluminum. This is in large part due to the drastic drop in temperature after the initial point for the second trial of the thermal electric cooler. Most probably, the data was skewed by the infrared thermometer used to measure temperatures. Since the thermometer could not be placed directly over the aluminum bar at 0 inches, it had to be shot at an angle to measure the first two data points. The cone of the laser increases as the thermometer is used at a larger range according to its distance to spot ratio of 6:1. Thus, it is likely that the reading is measuring not only the aluminum bar at 0 inches, but also some of the Styrofoam wall itself. Nevertheless, the both trials show a marked improvement in temperature gradient over the heat sink alone. The water bath for the first trial was 3.0°C while the water temperature was measured at 1.0°C for the second trial. The first trial was measured while running the thermal electric cooler at half power, 7 V and 1.8 A. The second trial was performed at the full power of the thermal electric cooler; 14 V and 4.0 A. This increase in power, however, failed to drastically change the resulting cooling power. This can be accounted for by the limiting natural convection of the cold side of the thermal electric cooler with the air in the Styrofoam box. When a fan and heat sink was mounted on the cold side, performance improved dramatically. Also, the thermal electric cooler was mounted fully inside the box in the first experimental apparatus. This meant that the power required to operate the device also contributed to heating the box. For the second experimental design, the thermal electric device was mounted coincident with the Styrofoam wall so that the cold plate would be the only thing exposed to the air in the box.

The data for the second apparatus, presented below, all was taken when two 40 watt light bulbs were used as the heat source rather than two 100 watt bulbs. Figure 12 shows the data taken for the heat sink alone. The water bath temperature was 0.5°C for both sets of data

shown below, and the temperature of the water inside the Styrofoam box was 38.0 degrees and 41.5 degrees for the two trials respectively.

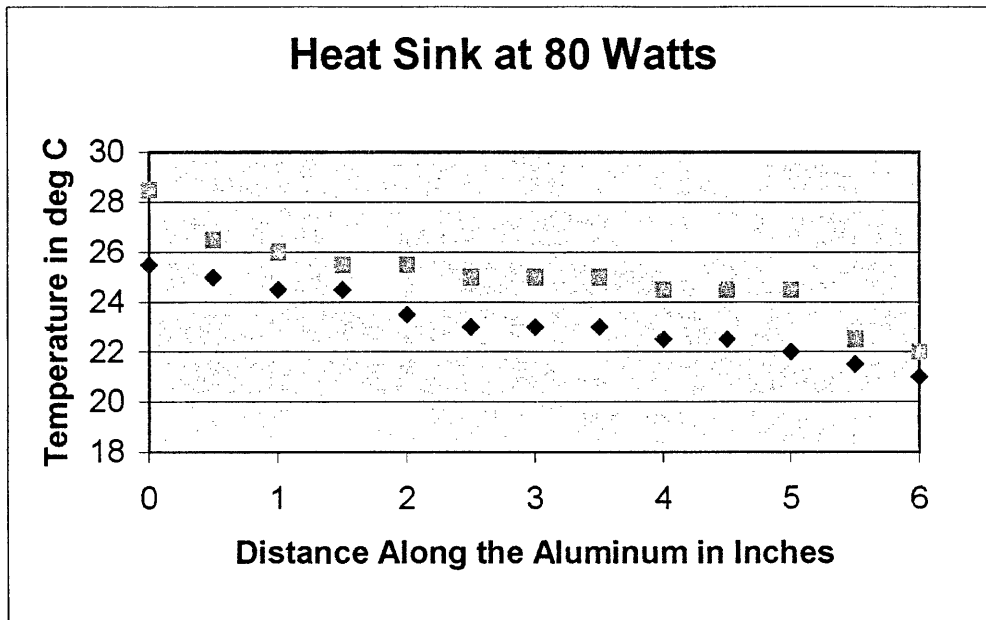


Figure 12: Heat sink data taken at 80 watts (second apparatus)

The figure shows a steady decrease in temperature down the length of the aluminum bar. The data for the two separate trials is similar in numerical value and nearly identical in slope. Compared to the data taken at 200 watts, this graph shows much more consistency. The second apparatus corrected several mistakes from the design of the first apparatus, resulting in less variation across the data sets

Figure 13 shows the data for the heat sink and fan combination using the second apparatus with two 40 watt bulbs. The fan was operated at the same voltage and current (12.0V and 0.15A) as the trials run using the first experimental apparatus. The water bath was 0.5°C for both trials while the water temperature inside the Styrofoam box was 39.5°C and 38.5°C for the two separate trials.



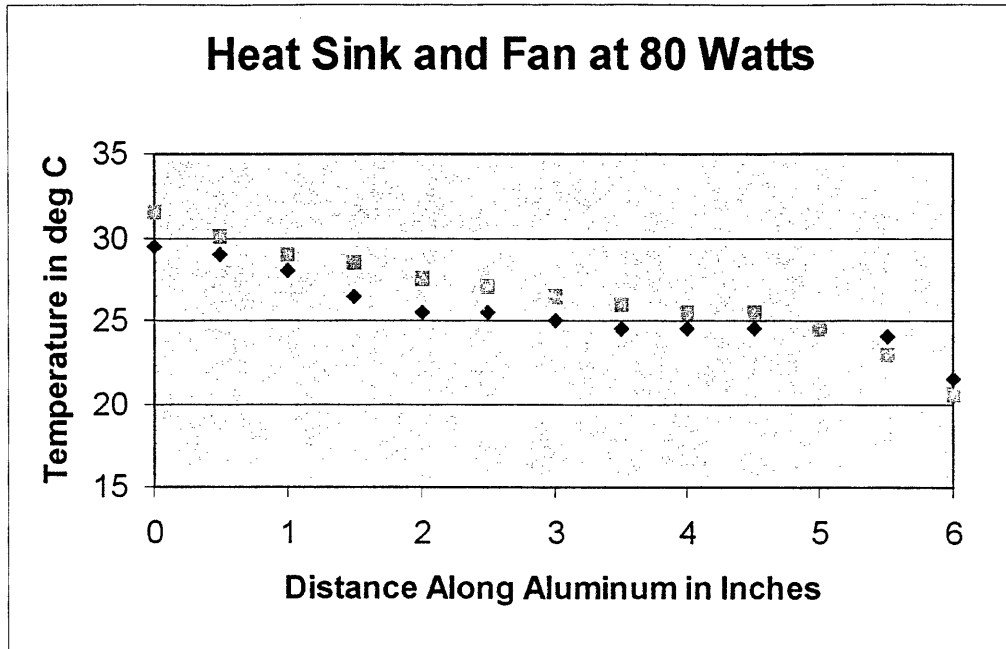


Figure 13: Heat sink and fan data at 80 watts (second apparatus)

This figure also shows the consistency of the second apparatus. The gradient across the aluminum still appears to have a sideways S shape to it, most likely caused by bad contact across joints, but the effect is limited compared to the first apparatus's data.

Figure 14 presents the one data set taken using the thermal electric cooler. The cooler was mounted in the wall of the Styrofoam and with a black heat sink attached to the cold side of the fixture. The Panaflo fan was used to blow hot air over the black heat sink. The device operated at 14.8 volts and 3.95 amperes for the duration of the trial. The water inside the box was measured at 37.0°C while the water bath had a temperature of 0.5°C.

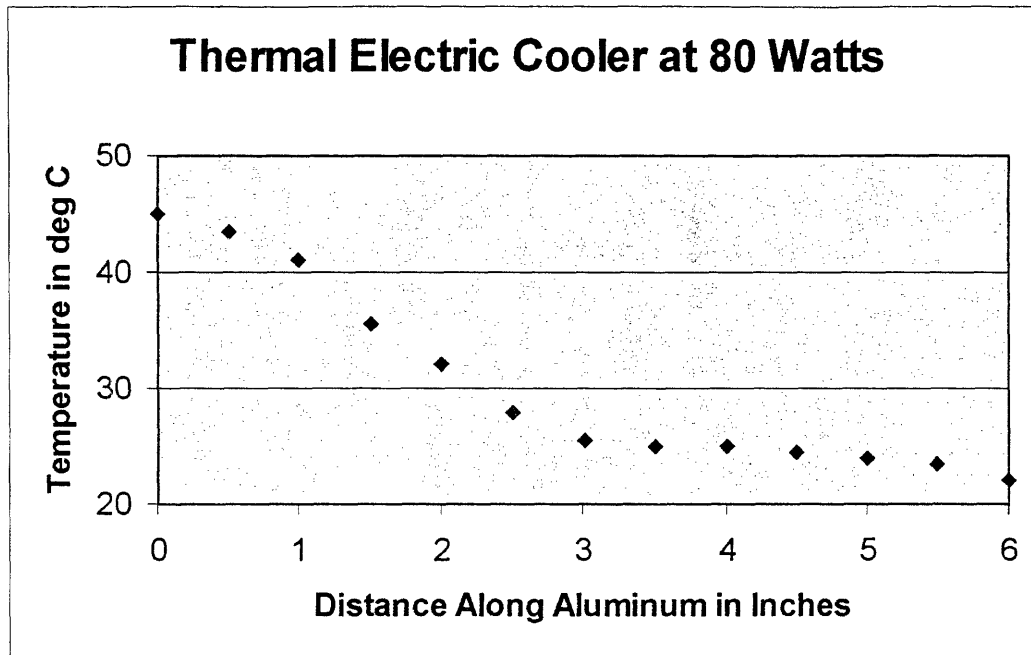


Figure 14: Thermal electric cooler data at 80 watts (second apparatus)

This data shows a marked difference from the thermal electric cooler data taken with the first apparatus. By mounting the thermal electric device in the same plane as the Styrofoam wall, the power consumption of the thermal electric device did not increase the air temperature inside the cooler as much. Also, by mounting a heat sink on the cold side of the fixture and running air across it with the fan, greater heat transfer rates were created and the device's potential was more fully utilized. The high temperature of the aluminum near the hot side of the device fixture shows that this potential was indeed being taken advantage of. The data levels off, however, at about 3 inches. This is likely due to the effects of convection and conduction to the packing foam on the aluminum. The leveling off occurred precisely where the thermal electric data set would have met up with the fan and heat sink data.

It is also important to remember, that even though this trial was measuring the cooling ability of the thermal electric cooler, there was heat transfer through the other heat sink and it was significant because the fan was circulating air throughout the box. There was no cold water bath for the other heat sink, but ambient air temperature provided enough of a gradient to notice temperature gradients across the aluminum.

## 6. Discussion

The theoretical model predicts an increase in the cooling power of the heat sink of 1.5 watts when used in conjunction with a fan. Using the calculated number, we can obtain an expected temperature gradient across the aluminum bar stock and compare it to the experimental data. Using the following equation:

$$Q' = k \cdot A \cdot (T_{\text{hot}} - T_{\text{cold}}) / L \quad (26)$$

and assuming an initial  $T_{\text{hot}}$  of 35°C based on the steady state condition and an assumed 0°C cold water bath, we get the following comparison, shown in Figure 15.

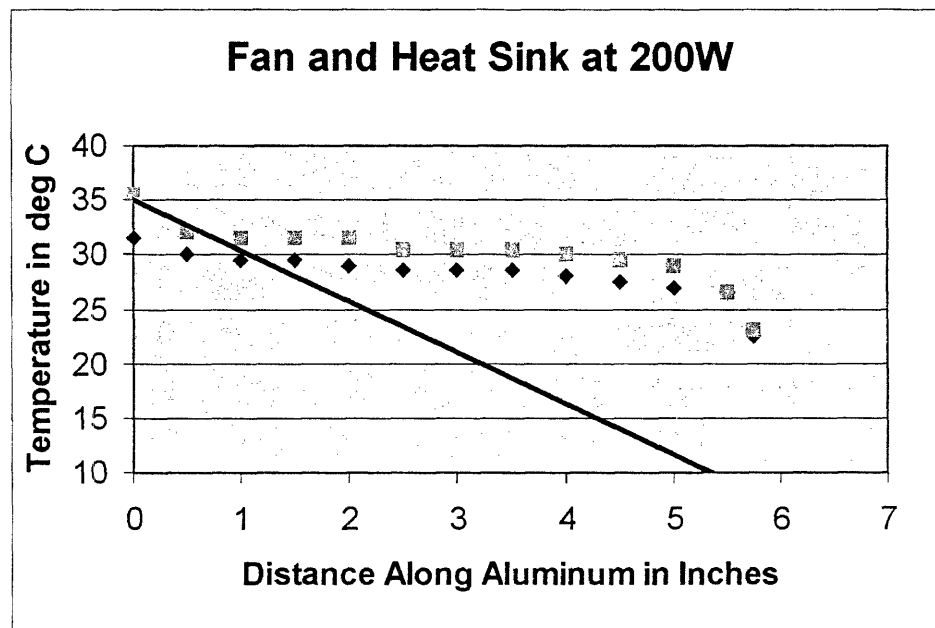


Figure 15: Overlay of theory on fan and heat sink data at 200 watts

It is clear that a linear temperature gradient is predicted by the theory. The experimental data does not agree with this, except in the middle section where the data seems to cut linearly across, but at a much smaller absolute slope. It is possible that the edges of the aluminum bar deviated from theory because of edge effects and the proximity to extreme temperature sources—the Styrofoam walls and the cold water bath. It is also likely that there was imperfect contact between the two pieces of aluminum, reducing the rate of heat transfer and the absolute value of the theoretical model's slope. Perhaps the largest loss, however, is convection. The horizontal aluminum bar was wrapped in packing foam to try and minimize natural convection with the ambient air in the room, but some of the bar had to be left exposed to measure. The horizontal bar was not wrapped in any foam.

The thermal electric cooler behaved below expectations. The device was limited in the 200 watt trials, however, by the lack of a fan blowing hot air across the cold side fixture. This left the cooler like an ice cube in a glass trying to cool a sauna. There needed to be some

airflow to take advantage of temperature gradient accomplished by the cooler. An overlay of the theory on the experimental data is shown below in Figure 16.

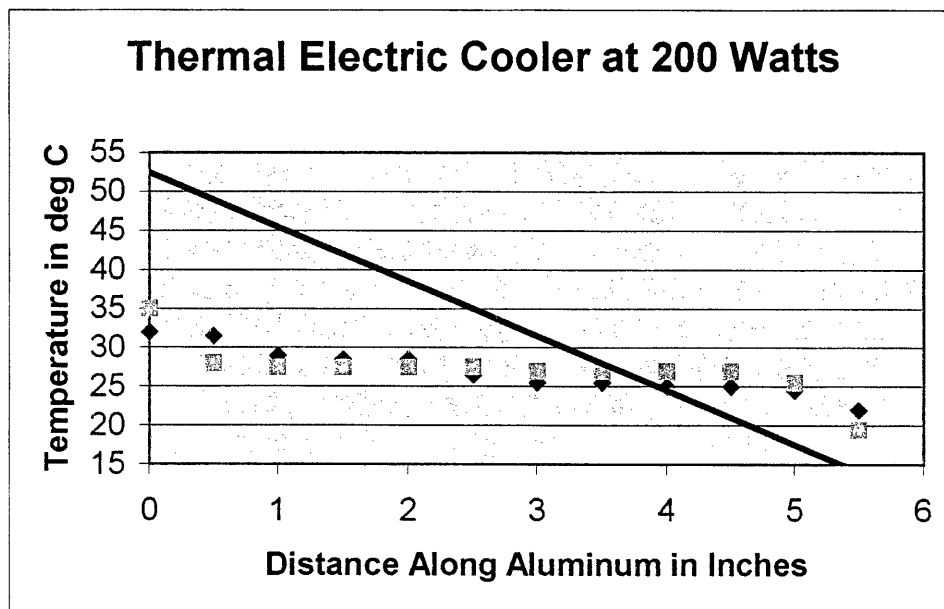


Figure 16: Overlay of theoretical prediction on thermal electric cooler data at 200 watts

Again, it is clear that the theory predicts a linear change in temperature across the aluminum bar. This corresponds to Fourier’s Law that describes pure conduction as linearly dependent on length of substance that is conducting the heat. The start temperature was determined from the current draw of the thermal electric cooler and the specifications found in Appendix A. The same losses and edge effects may be contributing the experimental behavior, but the biggest problem with the data is that the y intercepts of the graph are so different than the prediction. The experimental data shows a heat transfer rate of 15.9 watts while the theory predicted a value nearly three times as great. This is most likely due to the lack of air flow across the cold side plate inside the box as well as the fact that the 0 inch measurement was in reality, over 1 inch away from the thermal electric device. The fixturing of the cooler has bolt heads that kept the aluminum bar from protruding all the way out of the box. Also, the Styrofoam wall has a thickness of 1 inch, which is not accounted for in the x-axis values. These things were corrected for in the second building of the experiment by countersinking the bolts into the Styrofoam and by including an offset in the aluminum bar measurements.

A simple calculation of the coefficients of performance (COP) is important to the choice of cooling method for the satellite. On a spacecraft, electrical power comes at a premium. The fan was able to increase the cooling rate of the heat sink from 5.3 watts to 7.5 watts while only consuming 1.8 watts of electrical power. Calculating the COP using the following formula,

$$COP = Q'_{out} / Q'_{electrical\ in} \quad (27)$$

the COP of the fan and heat sink combination was 4.17. Performing the same calculation on the thermal electric device, which consumed 7.0 volts at 2.0 amps during the first trial, a COP

of 1.14 is obtained. This indicates that the fan and heat sink combination is superior in efficiency to the thermal electric cooler even if it cannot achieve as great a rate of heat transfer.

The corrections made for the second apparatus greatly improved the accuracy and reliability of the theoretical modeling. By measuring the temperature difference across the aluminum T-joint, an approximation of the thermal resistance could be found.

$$(T_{\text{hot}} - T_{\text{cold}}) / Q' = R_{\text{joint}} \quad (28)$$

Even though thermal grease was applied between the aluminum pieces, and the surfaces were sanded to make them as smooth as possible, a 5°C disparity existed between the ½ inch above the interface and below it. Perhaps 1°C of this can be attributed to conduction, so the ΔT that is used for equation 25 is 4°C. Using the Q' of 7.5 watts from the data above, the thermal resistance of the joint is found to be  $R_{\text{joint}} = .533 \text{ } ^\circ\text{C/W}$ . A natural convection loss can also be quantified using the same process shown in equations 5 through 11. Plugging in the conditions of the experimental apparatus,  $h_c$  is calculated out to 63.6 and an  $R_{\text{conv}}$  to 1.35  $^\circ\text{C/W}$ . If we assume that the interface between heat sink and aluminum bar has the same  $R_{\text{joint}}$  as the two aluminum bars have with each other, than a new model can be created taking these modifications into account. The new equivalent resistance,  $R_{\text{eq}} = 4.80$ , produces a heat transfer rate through the aluminum bar of  $Q' = 7.91$  watts considering the ΔT of 38°C as measured from water inside Styrofoam box to cold bath. Using this improved theory and overlaying the prediction with the data produces Figure 17, shown below, for the heat sink alone with two 40 watt bulbs.

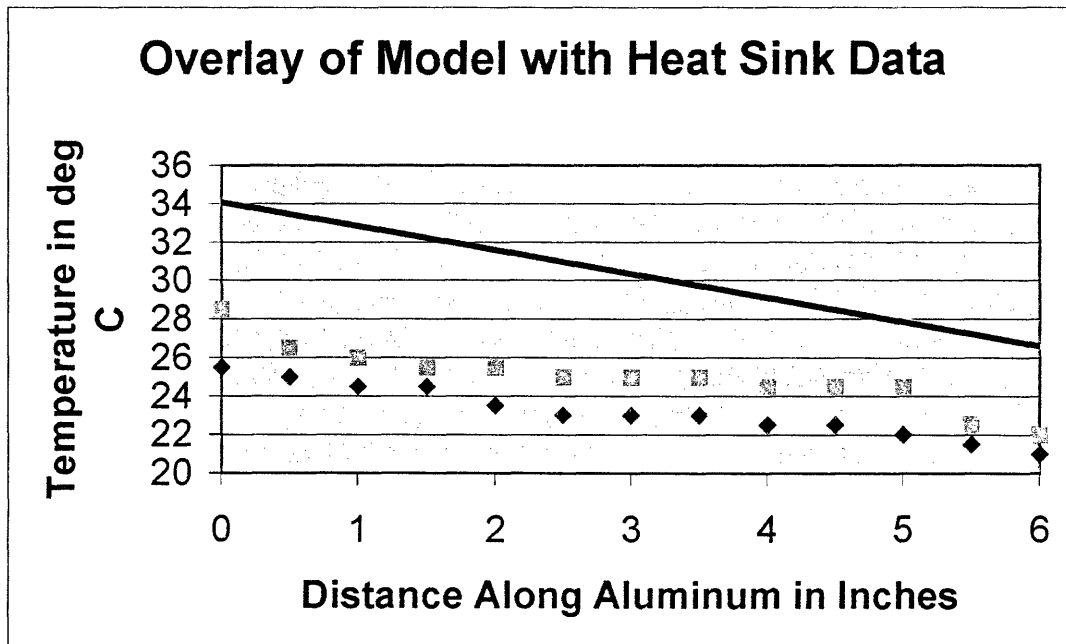


Figure 17: Overlay of model on heat sink data for the second apparatus at 40 watts

This prediction is clearly much more accurate than the model represented in Figure 14. The slope for this model is much closer to the actual data, based on a better number for the heat transfer rate,  $Q'$ , through the aluminum.

For the heat sink and fan, the same losses were factored into a new thermal resistance,  $R_{eq} = 3.66 \text{ }^\circ\text{C/W}$ . This corresponded to a new  $Q'$  of 9.73 watts. Using this number when overlaying the model on the heat sink and fan data produced Figure 18, below.

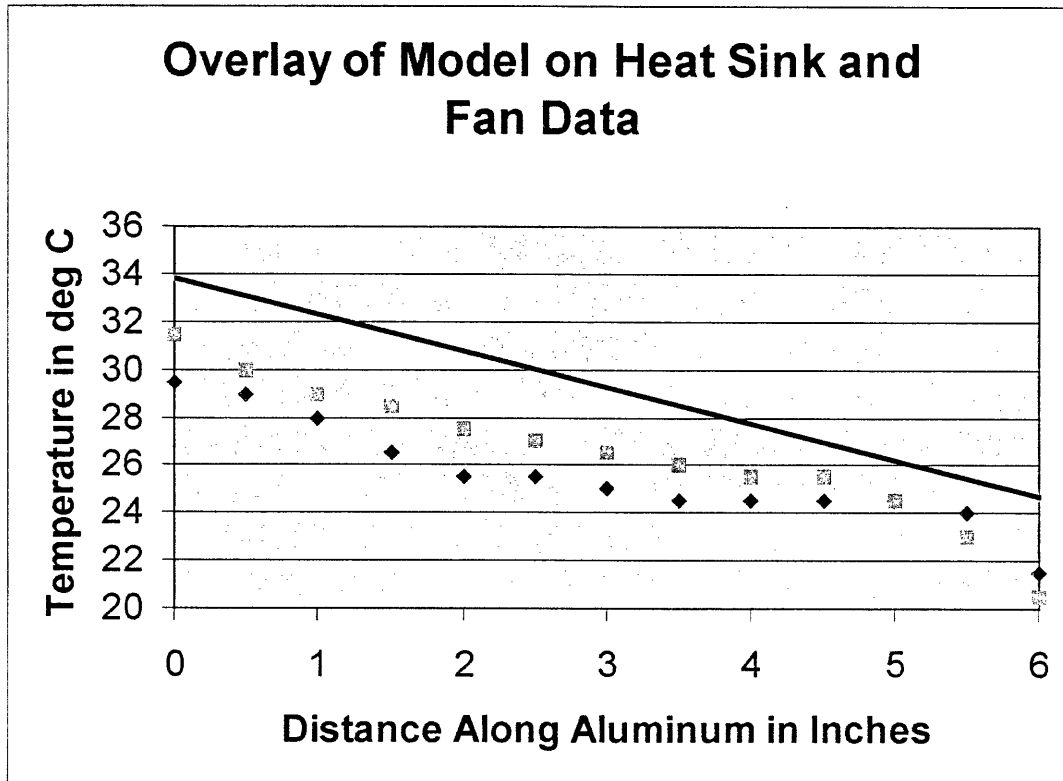


Figure 18: Overlay of model on heat sink and fan data; second apparatus at 40 watts

This graph shows a similar accuracy with the data as the previous prediction, Figure 17. The slope of the line, affected by the value of  $Q'$ , matches the data quite well. There is a slight upwards offset that might be attributed to a radiation loss term that is equal across the entire length of the bar. This model is much more useful for predicting the effects of fans in the payload capsule than the model developed for the first apparatus.

Figure 19 is the third overlay of theoretical analysis on experimental data. It shows the thermal electric trial along with the predicted behavior.

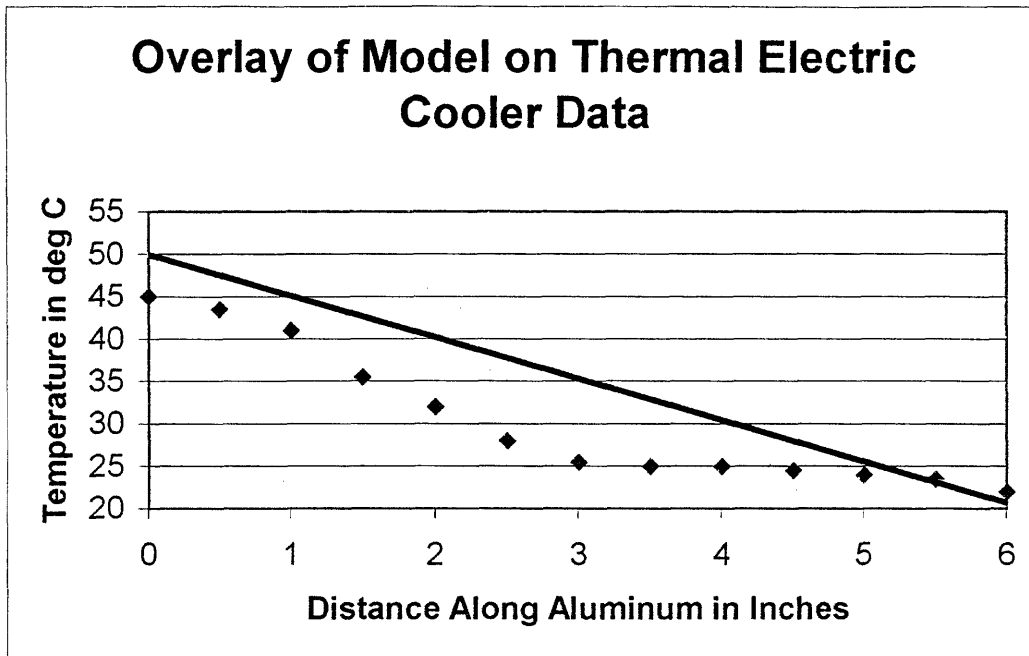


Figure 19: Overlay of model on thermal electric cooler data; second apparatus at 40 watts

This figure shows a huge improvement to Figure 16. However, it is interesting that it is mostly the data that has improved in this case, and not the model. The slope of the model is virtually unchanged, only a half volt voltage change was added to the power in. The reason that the data is so much closer, though, is due to all the changes in the apparatus between the first build and the second. By putting the thermal electric cooler in line with the wall and accounting for the aluminum bar stock that was formerly inside the cooler due to the bolt heads, the temperature readings improved dramatically. There are still some effects that are not being accounted for by the model, as seen near 2.5 inches where the data appears very much to be non-linear. Still, this model is a huge improvement and will be useful in comparing thermal electric devices to fans and heat sinks for use in the actual payload module.

Reevaluating the COP's for the devices using the new data from the second apparatus gives a COP of the fan and heat sink combination of 5.89. The COP of the thermal electric cooler in the new apparatus was 1.67 for operating at half power. So despite expectations, the fan increased performance far more efficiently than the thermal electric cooler. However, a fan has limitations on how much heat in can pump out of a system, therefore if a high load needs to be transferred, a thermal electric cooler might be a better solution because it is powerful, if not efficient.

Analyzing the error between the models and the actual experimental data is interesting. The first models, differed from the actual data by over 70% in some places. This error was in the form of an overshoot near the wall of the Styrofoam and as an undershoot when the temperature readings were taken near the cold water bath. The second set of models, on the other hand, only averaged errors of about 10% for the thermal electric cooler data and for the heat sink and fan data and 20% for the heat sink alone data. This error was consistently an overshoot for the entire length of the bar and was roughly in the form of a 2-

3°C offset. This might be corrected by adding a radiation term. Even though the emissivity of the aluminum used is only 0.1 or 0.2, this would bring the model noticeably closer still to the actual data.

There were also some errors within the data itself. The noncontact infrared thermometer only promises accuracy to plus or minus 2°C. The difficulty of measuring the temperature right next to the Styrofoam wall was discussed earlier as well in terms of the distance to spot ratio (6:1) of the device. The first apparatus certainly had considerably more sources of error due to the Styrofoam melting, the black plastic handles conducting heat out of the box, and the lack of proper circulation for the thermal electric cooler data. This error is hard to quantify because there was no measure of the Styrofoam's melting and evaporation rates.

If a more robust version of this experiment were to be undertaken, it would be wise to mount thermocouples or thermistors along the aluminum bar rather than trying to use a noncontact thermometer. The noncontact might still be used to measure Styrofoam wall temperature or the temperature of the water inside and outside the box, but using it on the aluminum is non-ideal.



## 7. Conclusions and Recommendations

After building and testing the first experimental apparatus with two 100 watt light bulbs, several problems were discovered. These design mistakes were analyzed and modified in the second building of the experiment. This second apparatus provided much more consistent data and never reached dangerous temperatures where melting and evaporation were issues. A theoretical model was developed accounting for all of the quantifiable losses except for radiation. The resulting fits were very similar to the data, but offset above the measurements by several degrees Celsius.

From section 5, *Results*, and 6, *Discussion*, it was clear that the fan and heat sink combination was much more efficient than the thermal electric cooler. However, the thermal electric cooler has its place and application as well. The fan was efficient, but did not export as much raw wattage as the thermal electric device. In the Mars Gravity application, a set amount of heat (80 watts on average) must be radiated into space if the mission is going to be successful. This is unachievable by the small scale fan and heat sink combination tested in the experiment. A very large velocity of air would have to be blown across many heat sinks set in parallel around the base of the payload capsule. Alternatively, a more expensive, but more efficient Peltier effect cooler might be used in the satellite. FerroTec Inc. makes such custom coolers for aerospace devices and can be hired to build a thermal electric cooler to specifications.

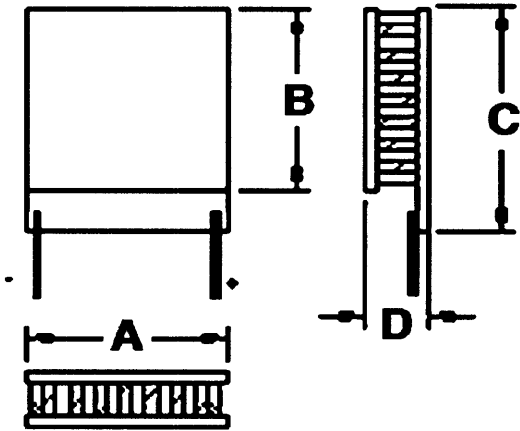
The experiment also revealed some other obstacles in designing the thermal system of the satellite. For instance, several sizable thermal resistances were calculated due joints in the structure. There are several interfaces in the thermal pathway that has been proposed for the Mars Gravity Biosatellite. To minimize the size of these  $R_{\text{joint}}$ 's, thermal grease should be used. The problem is that in space, thermal grease must have a no bleed characteristic; the grease must have practically zero vapor pressure. This eliminates all of the silicon-based greases that are used most commonly for this type of application. A list of alternative thermal vacuum gels is given in Appendix E.

The next step in the process of thermal design for the Mars Gravity Biosatellite is a plan and mock up of the actual system. Correct materials and dimensions should be used and a solid number for the lightband temperature should be obtained from the University of Washington team. Planetary Systems Inc., the manufacturer of the lightband, has offered to allow the Payload team access to its thermal vacuum chamber to conduct these tests. A more accurate thermal resistance of the lightband can then be obtained, and the control circuit for the payload module can be tested and modified accordingly. The controller will most likely have to regulate the voltage supplied to a thermal electric device and a fan and the sensor and feedback loop must be constructed and tested.

After a working model with correct dimensions, materials, and sensors has been built and tested, the collaboration of all the payload mock-ups must take place. The atmospheric, cage design, thermal system, structural placements of elements, and scientific experiments will have to be coordinated into one full size test and run for the full length of the mission with live mammal subjects. If this goes successfully, the final construction of the satellite will be contracted out and manufactured before a final round of testing and pre-launch preparations. This experiment provides the basic investigation of principles that will be used for comparison and understanding all the way up the design chain to their eventual implementation in the final, launchable, Mars Gravity Biosatellite.

## 8. Appendix A

The specifications sheet for the Melcor thermal electric cooler is pasted below.



Leads		I <sub>max</sub> (Amps)	Th = 25° C			N	Dimensions (mm)			
Inches	Wire Gauge (awg)		Q <sub>max</sub> † (Watts)	V <sub>max</sub> (Volts)	Delta T <sub>max</sub> (°C)		A	B	C	D
6	18	8.5	72	14.4	64	127	40	40	44	3.3

†Q<sub>max</sub> rated value at delta T = 0°, I<sub>max</sub> and V<sub>max</sub>, Th = 25° C.

## Appendix B

Shown in table 1 below is the raw data for two trials of the heat sink functioning alone. Two 100 watt light bulbs were in the system.

distance along aluminum in inches	heat sink trial 1	heat sink trial 2
0	24.5	32.5
0.5	24	33.5
1	23.5	29
1.5	23.5	29
2	23.5	28.5
2.5	23.5	28
3	23.5	28
3.5	23.5	27.5
4	23.5	27
4.5	23	27
5	22.5	26.5
5.5	22	26
5.75	19	22

Table 1: Data for heat sink alone in first experimental apparatus with two 100 watt light bulbs

Table 2 shows the data for the rebuilt apparatus run with two 40 watt light bulbs.

distance along aluminum in inches	heat sink alone trial 3	heat sink alone trial 4
0	25.5	28.5
0.5	25	26.5
1	24.5	26
1.5	24.5	25.5
2	23.5	25.5
2.5	23	25
3	23	25
3.5	23	25
4	22.5	24.5
4.5	22.5	24.5
5	22	24.5
5.5	21.5	22.5
6	21	22

Table 2: Data for the heat sink alone in the second experimental apparatus with two 40 watt light bulbs

## Appendix C

Shown below in table 3 is the raw data for the heat sink and fan combination operating when two 100 watt light bulbs were used.

distance along aluminum in inches	Fan and Heat Sink	
	Fan and Heat Sink trial 1	Fan and Heat Sink trial 2
0	31.5	35.5
0.5	30	32
1	29.5	31.5
1.5	29.5	31.5
2	29	31.5
2.5	28.5	30.5
3	28.5	30.5
3.5	28.5	30.5
4	28	30
4.5	27.5	29.5
5	27	29
5.5	26.5	26.5
5.75	22.5	23

Table 3: Raw data for the fan and heat sink combination taken using the first apparatus run with two 100 watt light bulbs

The following table, Table 4, shows the data for the fan and heat sink in the second experimental apparatus.

distance along aluminum in inches	heat sink and fan	
	heat sink and fan trial 3	heat sink and fan trial 4
0	29.5	31.5
0.5	29	30
1	28	29
1.5	26.5	28.5
2	25.5	27.5
2.5	25.5	27
3	25	26.5
3.5	24.5	26
4	24.5	25.5
4.5	24.5	25.5
5	24.5	24.5
5.5	24	23
6	21.5	20.5

Table 4: Raw data for the fan and heat sink as part of the second apparatus. Two 40 watt light bulbs were used.

## Appendix D

Shown below in Table 5 is the raw data for the thermal electric cooler experiment when two 100 watt light bulbs were providing the heat source.

distance along aluminum in inches	thermal electric cooler	thermal electric cooler
	trial 1	trial 2
0	32	35
0.5	31.5	28
1	29	27.5
1.5	28.5	27.5
2	28.5	27.5
2.5	26.5	27.5
3	25.5	27
3.5	25.5	27
4	25	27
4.5	25	27
5	24.5	25.5
5.5	22	19.5

Table 5: Raw data for the aluminum bar stock attached to the thermal electric cooler; first apparatus, two 100 watt light bulbs

The next table is the raw data which was also taken for the thermal electric cooler trials, but using the second apparatus and two 40 watt light bulbs.

distance along aluminum in inches	thermal electric cooler trial 3
0	45
0.5	43.5
1	41
1.5	35.5
2	32
2.5	28
3	25.5
3.5	25
4	25
4.5	24.5
5	24
5.5	23.5
6	22

Table 6: Data from the thermal electric cooler trial using the second apparatus, two 40 watt light bulbs

## Appendix E

Below is a list of thermal grease vendors and descriptions of thermal greases that have the potential to be used in aerospace applications. They are all silicon free and have no bleed guarantees.

Sil-Free grease	<a href="http://www.aavidthermalloy.com">www.aavidthermalloy.com</a>
Custom Grease Manufacturing	<a href="http://www.dowcorning.com">www.dowcorning.com</a>
Krytox vacuum lubricant (Dupont)	<a href="http://www.ee.ualberta.ca/~schmaus/vacf/vacmat.html">www.ee.ualberta.ca/~schmaus/vacf/vacmat.html</a>
Cryo-application vacuum grease Apiezon N Grease (\$152/25g)	<a href="http://www.proscitech.com.au/catalogue/">www.proscitech.com.au/catalogue/</a>  <a href="http://www.santovac.com">www.santovac.com</a> (636) 723 0240